

Tumour oxygenation measurements by ^{19}F magnetic resonance imaging of perfluorocarbons

Dominick J. O. McIntyre*, Cheryl L. McCoy and John R. Griffiths

CRC Biomedical MR Research Group, St. George's Hospital Medical School, London, SW17 0RE, UK

Solid tumours are well known to be heterogeneous and contain a significant fraction of hypoxic cells, which are protected against the effects of radiotherapy. A non-invasive method for measuring tissue oxygenation would therefore be useful. The ^{19}F magnetic resonance signals from perfluorocarbons are sensitive to oxygen concentration. We have used this property to measure tumour oxygenation of the GH3 prolactinoma, RIF-1 fibrosarcoma and SaF sarcoma in mice by fluorine magnetic resonance imaging (MRI) of intravenously injected perfluorocarbons which are taken up by macrophages in the tumour. We have also studied the injection of perfluorocarbons directly into the tumour, which allows less of the tumour to be studied but has a higher success rate and gives values more consistent with Eppendorf polarographic electrode measurements.

It is well established that solid tumours are heterogeneous and that the hypoxia of tumour cells, caused by abnormal and/or poorly developed vasculature, protects against the effects of ionizing radiation¹. This hypoxia is due in part to rapid growth, which leads to inadequate and chaotic blood vessel development and thus to heterogeneity in the delivery of O_2 (and also other nutrients) to cells within the tumour. This has considerable significance for the efficacy of radiotherapy. A non-invasive method for detection of tissue $p\text{O}_2$ could thus be useful, in both the laboratory and the clinic.

Currently the classic way to measure tumour $p\text{O}_2$, both in animal² and patients³ is with fine needle O_2 electrodes. Eppendorf electrodes sample a few hundred microenvironments as they track across a tumour, giving a histogram from which mean and median $p\text{O}_2$ values for the tumour can be calculated⁴. These types of electrodes not only damage the tissue but also actually consume oxygen, and the effects of this may compromise the results. Because of these drawbacks, the search continues for less-invasive methods for measuring tumour oxygenation. One method that meets this criterion is based on fluorine magnetic resonance (^{19}F MR). The method uses ^{19}F MR to non-invasively measure $p\text{O}_2$ of a perfluorocarbon (PFC) *in situ*.

Perfluorocarbons are organic molecules in which the hydrogen atoms have all been replaced by fluorine atoms, hence giving a strong ^{19}F MR signal. Since there is no MR-visible fluorine native to the tissue, the signal to noise ratio (SNR) of PFC studies can be very high. PFCs have a great affinity for oxygen, dissolving a similar amount per unit volume to blood, and hence have been used both as blood substitutes and to supply oxygen directly to the lungs of experimental animals⁵. Additionally, they are biologically inert, non-toxic and some are commercially available both as liquids and as lipid emulsions. Recently PFCs have been developed for use in MR, which have all or most of the signal concentrated in a single resonance, simplifying the task of imaging. When PFCs are administered intravenously (i.v.) as a lipid emulsion, they are sequestered over a period of several hours into the reticulo-endothelial system, particularly in tissues with high levels of macrophages. This includes the liver and spleen, and also many tumours which can consist of up to 50% macrophages. Ever since it was shown that there is a linear relationship between the ^{19}F MR spin-lattice relaxation time ($R_1 \approx 1/T_1$) of PFC and $p\text{O}_2$ (ref. 6), there has been a developing interest in exploiting this phenomenon for measuring and monitoring tissue $p\text{O}_2$ using non-invasive ^{19}F MR⁷⁻⁹. Oxygenation maps can give information not only about the distribution of $p\text{O}_2$ across the microregions of the tumour but also a global (mean) measurement.

Recently, Sotak and co-workers developed a method using inversion recovery (IR) echo-planar ^{19}F magnetic resonance imaging (MRI) to generate $p\text{O}_2$ maps of perfluorocarbons in tumours and normal tissues¹⁰. With generous help and advice from Sotak, we have attempted to extend these studies. We modified his method in three ways: firstly by using the perfluorocarbon, Fluorovist (L13106; generously donated by Hema-gen, St. Louis, MO, USA) whose ^{19}F T_1 relaxation rate is sensitive to O_2 concentration; secondly by using a spin-echo sequence based on the SUFIR method of Canet *et al.*¹¹; and finally by enhancing the uptake of Fluorovist into the tumour by allowing the animals to breathe carbogen (95% O_2 /5% CO_2). Host carbogen breathing is thought to cause vasodilation of blood vessels in tumours¹², thus improving the access of PFC to

*For correspondence: (e-mail: d.mcintyre.sghms.ac.uk)

the tumour cells. These modifications allowed us to perform slice-selective T_1 imaging of the PFC in mice. Even with carbogen breathing, the tumours do not always take up PFC, and its access to poorly-vascularized regions is restricted. To sidestep these limitations, we also injected PFC directly into the tumours (i.t.). In general, we found it difficult to reproduce some of the results of the Sotak group, possibly because of differences in tumour models. However, tumour pO_2 distribution was successfully measured both with the i.v. and i.t. administration methods, and the results obtained have interesting implications concerning the distribution of cellular oxygenation in tumours.

Methods

Animals

RIF-1 tumours were grown subcutaneously on the flank of C₃H mice according to the method of Twentyman *et al.*¹³. GH3 prolactinomas were grown subcutaneously on the flank of nude (Nu/Nu) mice, which were maintained under standard conditions as previously described¹⁴. SAF tumours were grown subcutaneously on the lower dorsum of syngeneic CBA/Gy f TO mice and maintained as previously described². The C₃H mice were anaesthetized with a single intraperitoneal (i.p.) injection of a combination of fentanyl citrate (0.315 mg/ml) plus fluanisone (10 mg/ml ('Hypnorm', Janssen Pharmaceutical Ltd.), midazolam (5 mg/ml) ('Hypnovel', Roche) and water (1:1:2), at a dose of 10 mg/kg and the nudes with i.p. injections of ketamine ('Ketalar', Park-Davis Pharmaceuticals) (45 mg/kg) and diazepam (Phoenix Pharmaceuticals, Ltd.) (20 mg/kg). Tumour size was determined from the formula $\pi/6 d_1 d_2 d_3$ where d_1 , d_2 and d_3 were the three orthogonal dimensions of the tumour. Tumours were selected at volumes of 500 to 700 mm³ for the initial measurements. When tumours were examined on subsequent occasions (up to 4 days), the volumes had increased to between 700 and 1500 mm³.

PFCs used

Fluorovist (also known as L13106) and perfluorocarbon-15-crown-5-ether (PCE) were donated by HemaGen, St Louis, Mo, USA, and hexafluorobenzene (HFB) was purchased from Sigma. Fluorovist and PCE were supplied as lipid emulsions for i.v. or i.t. injections. The emulsions were composed of 58% v/v water, 2% oil and 40% perfluorocarbon, with an average particle size of 200 nm. Fluorovist was also supplied as a pure liquid, as was HFB; unemulsified, pure liquids were used for i.t. injections only. Fluorovist and PCE are commercial PFCs designed for MR use. They have relatively short

T_1 's. Additionally, the ¹⁹F MR spectrum of PCE contains only one peak, and that of Fluorovist contains two peaks very close together with similar T_1 values at all O₂ concentrations. HFB, like PCE, has only a single resonance. Its T_1 is 2–3 times longer than that of PCE or Fluorovist at a given pO_2 , thus requiring a longer imaging time for a given SNR to be obtained. Its T_1 changes less with temperature than do those of PCE and Fluorovist, reducing the potential errors in pO_2 measurement.

The O₂ sensitivity of the perfluorocarbons was measured by bubbling a vial for 20 min with gases containing 0%, 18% and 95% O₂, then measuring T_1 using both inversion recovery spectroscopy and the superfast inversion recovery (SUFIR) imaging sequence described later in this article. The two methods agreed to $\pm 10\%$.

Administration protocols

Intravenous injections (i.v.). Injections of either Fluorovist or PCE as follows: 9 mmol/kg PFC alone, MRI on one occasion between 1 and 4 days from injection; 9 mmol/kg PFC + carbogen, MRI on one occasion between 1 and 4 days from injection; 9 mmol/kg PFC + carbogen on day 1, repeated on day 2, MRI day 4; 4.5 mmol/kg PFC + carbogen on day 1, repeated on day 2, MRI day 4.

Where carbogen was given, the animal breathed the gas at a rate of 2 l/min for 15 min immediately after the injection of the PFC, a strategy intended to increase the quantity and uniformity of the PFC uptake in the tumours by enhancing the blood flow while the PFC content of the bloodstream was highest.

Intratumoural injections (i.t.). In some experiments, 20 μ l of emulsified HFB was injected directly into the tumour using a Hamilton syringe with a 25-G (5/8") needle. In others 3 \times 15 μ l droplets of pure, unemulsified HFB or Fluorovist were injected. Multiple injections were given to reduce the chance of PFC leakage and to allow tumour heterogeneity to be studied. All animals were scanned within 15 min of injection. Some were followed up over a few days to investigate any changes after i.t. injection.

Blood flow modification

Two blood flow modifiers were used. Carbogen (95% O₂/5% CO₂) is thought to cause vasodilation of tumour blood vessels, enhancing blood flow and tumour oxygenation. Carbogen was used in two distinct roles: firstly, it was administered for 15 min at a rate of 2 l/min immediately after i.v. injection of PFC to increase the quantity of blood-borne PFC flowing through the tumour, with the intention of enhancing the level of

uptake; secondly, it was administered at a rate of 2 l/min during the MRI examination to investigate whether it caused an increase in tumour oxygenation which could be detected by ^{19}F T_1 imaging. The effects of carbogen are transient, so its use after injection should have no effect on an MRI experiment performed 24–96 h later. In some cases, 1000 mg/kg nicotinamide (Sigma) was also administered during the MRI examination, as this compound is thought to decrease transient blood vessel closure¹⁵. Again, the intention was to investigate whether an increase in oxygenation could be detected.

Magnetic resonance

A 33 cm bore 1.9 T SMIS spectrometer equipped with shielded gradients of peak strength 4 G/cm was used. For some of the i.v. administered PFCs, a 3 cm birdcage coil double-tuned to ^{19}F and ^1H was used; a surface coil of diameter 19 mm detunable from ^{19}F to ^1H was used for the other i.v. experiments and for all the i.t. experiments.

Non-localized spectroscopy (MRS) gives higher sensitivity and finer time resolution than imaging, allowing successful studies to be made at lower levels of PFC than MRI, while imaging allows the whole animal to be studied, distribution of PFC in different organs to be analysed, and tumour heterogeneity to be examined. We therefore chose to perform imaging studies. Sotak and co-workers¹⁰ used inversion-recovery echo-planar imaging (EPI) of PCE to obtain O_2 maps of normal and tumour tissue in mice. They reported $p\text{O}_2$ values of 26 mm Hg from their RIF-1 tumours. Their tumour images were projections through the entire tumour, since the SNR was not high enough for slice selection. Consequently, we chose to use a slower imaging sequence which gave higher SNR, and allowed slice selection.

We implemented an imaging sequence based on the SUFIR method of Canet *et al.*¹¹, which is a localized version of a simple and accurate method for obtaining T_1 values by spectroscopy. The sequence is shown in Figure 1. An adiabatic hyperbolic secant pulse, which reduced the sensitivity to RF amplitude errors, was used for the inversion pulse. For surface coil experiments, a B_1 -insensitive saturation sequence comprising 3 adiabatic half-passage pulses followed by gradient blips along the three axes was used. Two images were obtained with different saturation factors, allowing T_1 to be calculated at each point from the formula $T_1 = -T_{ip}/\ln(1 - (S_2/S_1))$, where T_{ip} is the inter-pulse delay and S_2 , S_1 are the amplitudes at the given point in the two images. For i.v. studies on Fluorovist experiments the T_{ip} was between 2.4 and 2.2 s, the field of view (FOV) 50 mm, the slice thickness 8 mm and the matrix size 64×64 . Six scans were used for an imaging time of 45 min. Parameters used for i.t. studies on Fluorovist

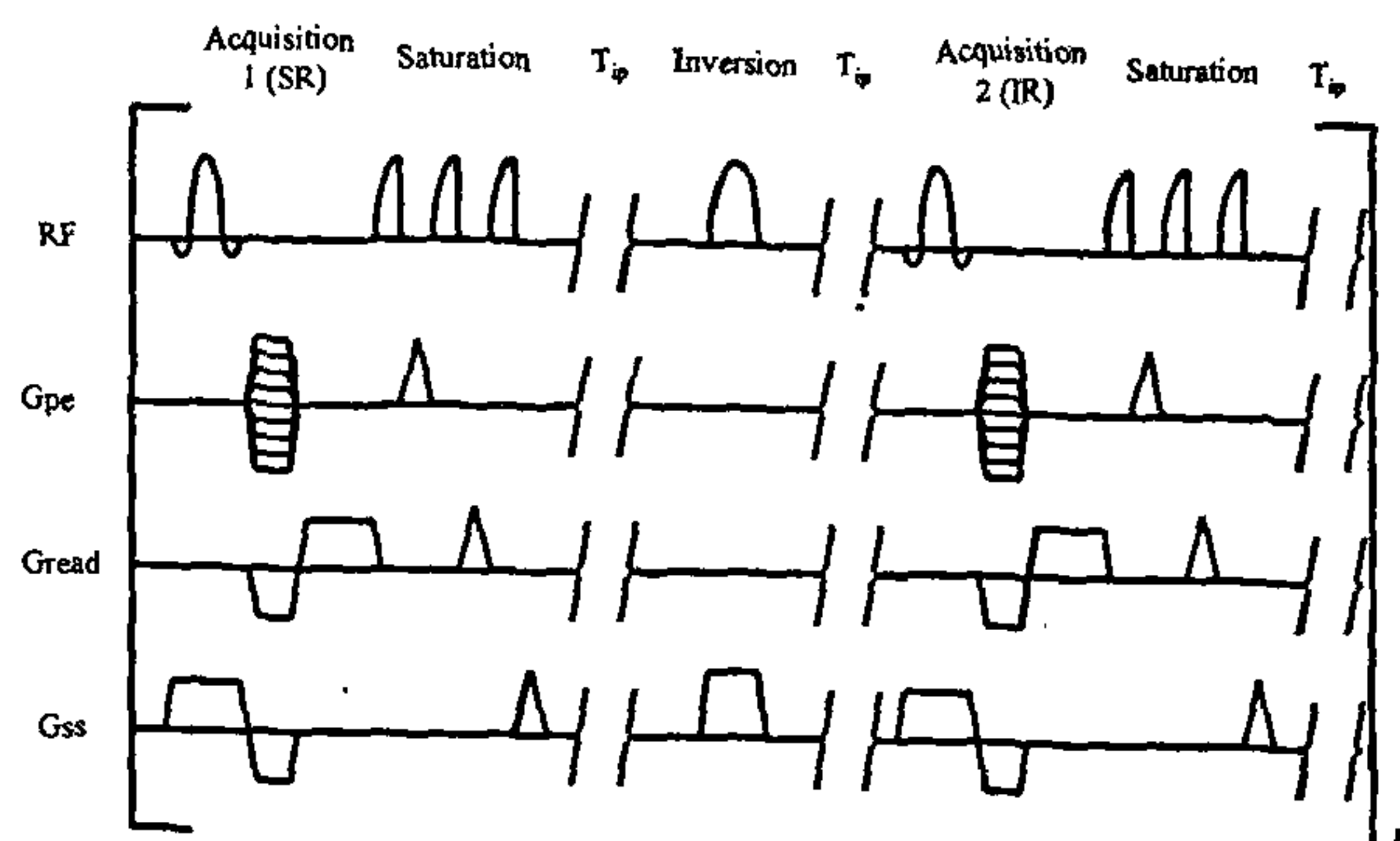


Figure 1. The SUFIR imaging sequence. This generates two differently T_1 -weighted images. The first is a saturation recovery image after the magnetization has recovered for a time T_{ip} . The magnetization is then saturated, allowed to recover for T_{ip} , inverted and allowed to recover for a further time T_{ip} , when a second image is obtained. The magnetization is then saturated again and the sequence repeated for the next phase-encoding step. An adiabatic inversion pulse was used. For surface coil experiments, adiabatic saturation pulses were also used to minimize errors due to RF inhomogeneity.

were: an inter-echo time of 1.5 to 1.8 s, on FOV of 35 mm, 64×32 points and 4 averages giving an imaging time of 11 min. For i.t. experiments on HFB, an inter-echo time of 4.0 s, a FOV of 35 mm, 64×32 points and 2 averages giving an imaging time of 13 min, were used. The images were converted to $p\text{O}_2$ maps by a Visual C++ program run on the SMIS console. Regions of interest (ROIs) were selected from regions of high signal in the SUFIR images and the $p\text{O}_2$ values for each time point measured.

Three types of studies were performed: (i) baseline measurement only; (ii) baseline measurement followed by one image during which the animal was allowed to breathe carbogen, followed by a series of recovery images during which the animal breathed air freely; and (iii) the animal was allowed to breathe carbogen throughout the experiment, and nicotinamide was injected at the end of the first image. With carbogen breathing, a scavenger pump was used to prevent accumulation of carbogen in the magnet bore.

Results and discussion

T_1 measurements of pure perfluorocarbons and implementation of imaging sequences

The HFB calibration results obtained from spectroscopy are shown in Table 1. The slope and intercept were obtained by linear fitting in Origin (Microcal Software, Inc.). The Fluorovist calibration was based on results obtained by Sotak (personal communication) and verified in our laboratory.

Table 1. Relaxation times as a function of pO_2 for hexafluorobenzene at 20°C. When modelled as $R_1 = A + B \cdot pO_2$ using Origin (Microcal Software), with pO_2 measured in mm Hg, the values obtained were $A = 0.062 \pm 0.06 \text{ s}^{-1}$, $B = 3.54 \pm 0.14 \times 10^{-3} \text{ s}^{-1} \text{ mm Hg}^{-1}$

0% O_2		18% O_2		95% O_2	
T_1/s	R_1/s^{-1}	T_1/s	R_1/s^{-1}	T_1/s	R_1/s^{-1}
9.2	0.11	2.04	0.49	0.38	2.63

Measurements using crown ether PCE and Fluorovist

At the start of this project, only a small amount of emulsified PCE was available, and this was given to 2 mice bearing RIF-1 tumours. However, in contrast to the experience of Sotak *et al.*, little of the PCE was taken up into the tumours – typically 2–3% of that injected. Figure 2 *a* and *b* shows a proton scout image and the corresponding fluorine image. The increased ^{19}F intensity over the liver and spleen suggested that much of the PCE was sequestered in these two organs. Because of the difficulty in obtaining more PCE, Fluorovist was subsequently used. The results using Fluorovist were similar to those obtained with PCE. This is to be expected as both perfluorocarbons were administered as lipid emulsions of similar particle sizes. In 17 mice bearing RIF-1 tumours, the Fluorovist uptake into the tumour resulted in sufficient uptake for T_1 mapping of the tumour in only 5 cases, and never resulted in uptake both high and uniform. In trying to find the reasons for this lower uptake, we considered whether the RIF-1 tumours used in our laboratory could be different to those used by Sotak. Oxygen electrode measurements, performed by Collingridge using Eppendorf fine needle electrodes, indicated that median pO_2 of our RIF-1 tumours at 1.3 mm Hg¹⁶ is significantly lower than that measured by Sotak using MRI (26 mm Hg), suggesting that the vascularization of our tumours may be much poorer, rendering them less able to take up the PFCs.

Since low tumour blood flow appeared to be a possible cause of the differences between our results and Sotak's, we tried to enhance the blood flow by allowing the mice to breathe carbogen immediately after administration of the PFCs, to see if more PFC would be taken up by the tumours. PFC injections were performed on 42 mice (with 4 injection failures) as described in the methods. 10 tumours with high uptake (tumour SNR 30–70) and 28 tumours with poor uptake (SNR 0–30) were obtained.

In the tumours with satisfactory SNR, the PFC uptake was much more uniform than in the absence of carbogen breathing. In tumours where the SNR was between 0 and 30, too low for T_1 mapping, the PFC uptake was often still better than that obtained without carbogen breathing. The success of the enhancement was not correlated with

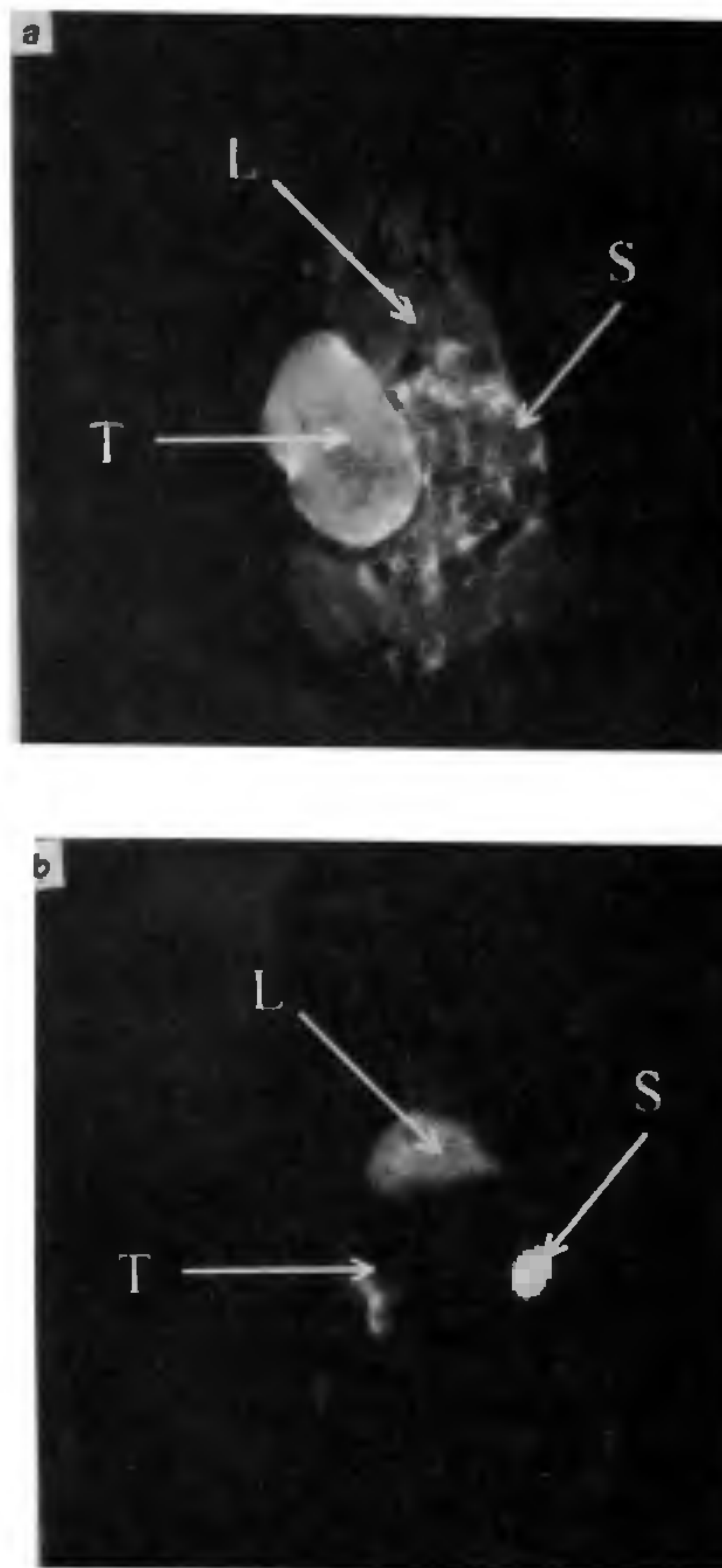


Figure 2. *a*, ^1H and *b*, ^{19}F whole-body images of a C_3H mouse bearing a RIF-1 tumour after i.v. administration of the perfluorocarbon PCE. Note the high intensity in liver and spleen, and the inhomogeneous uptake in the tumour in the ^{19}F image. The liver, spleen and tumour are labelled L, S and T respectively.

the size of the tumour (results not shown, $P < 0.1$). Proton scout images show dark lines in the tumours where the enhancement was successful; the tumours were relatively featureless when the PFC was not taken up (see Figure 3 *a, b* and Figure 4 *a, b* which show ^1H and ^{19}F images for low and high uptake respectively, and Figure 5 which shows the T_1 map and pO_2 map obtained from the ^{19}F image in Figure 4). This could either be due to high concentration of PFC reducing the proton signal in these areas, or to blood flow in large vessels washing out the signal. In the second case, proton imaging of the tumours prior to PFC injection should allow the PFC uptake to be predicted. A series of studies of this type failed to predict the PFC uptake, no dark lines being observed prior to PFC injection, and we therefore ascribed the dark lines to displacement of the water signal by high PFC uptake. When enough PFC was taken up for a T_1 map to be constructed, the mean pO_2 value was 44 ± 8 mm Hg in the 10 successful tumours. This is

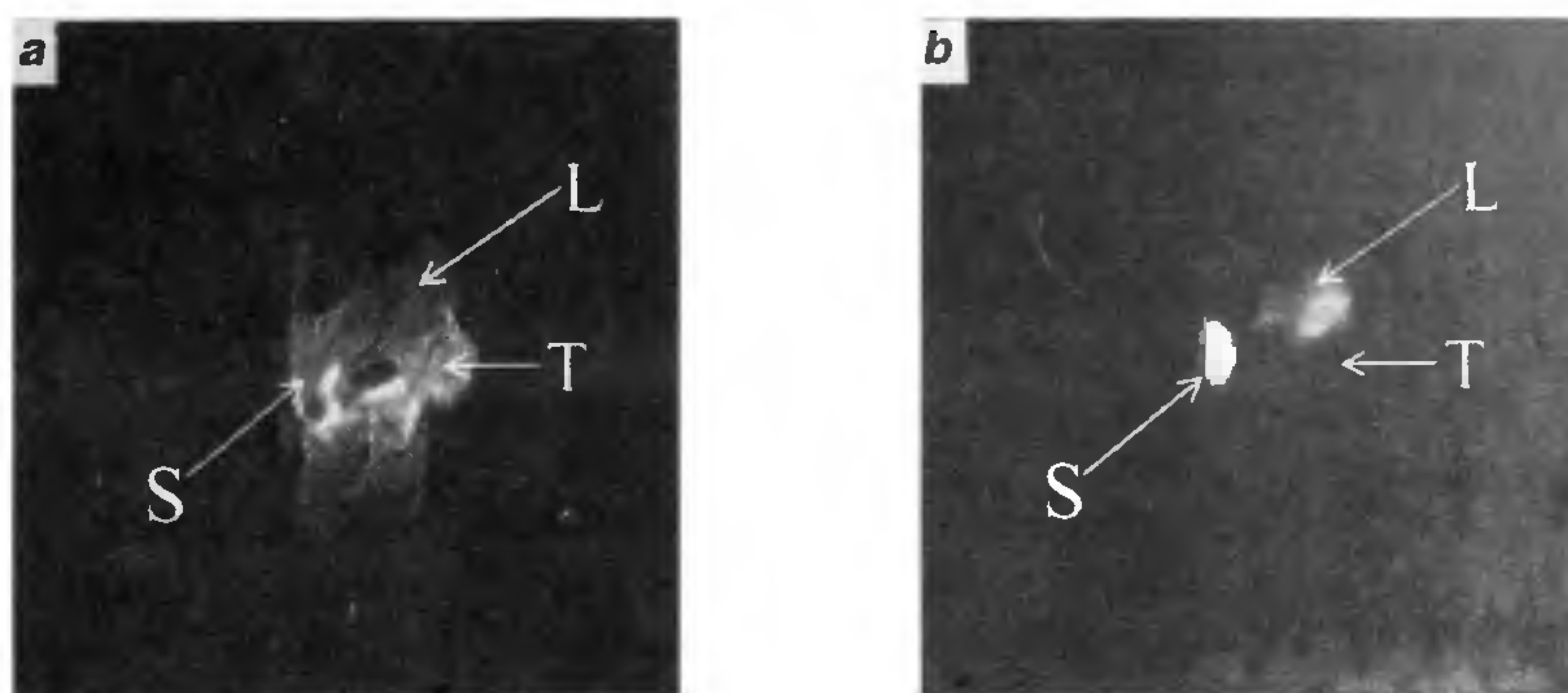


Figure 3. *a*, ^1H and *b*, ^{19}F whole-body images of a C_3H mouse bearing a RIF-1 tumour after i.v. administration of the perfluorocarbon Fluorovist. There has been no uptake in the tumour in the ^{19}F image, as is the case in 75% of such experiments.

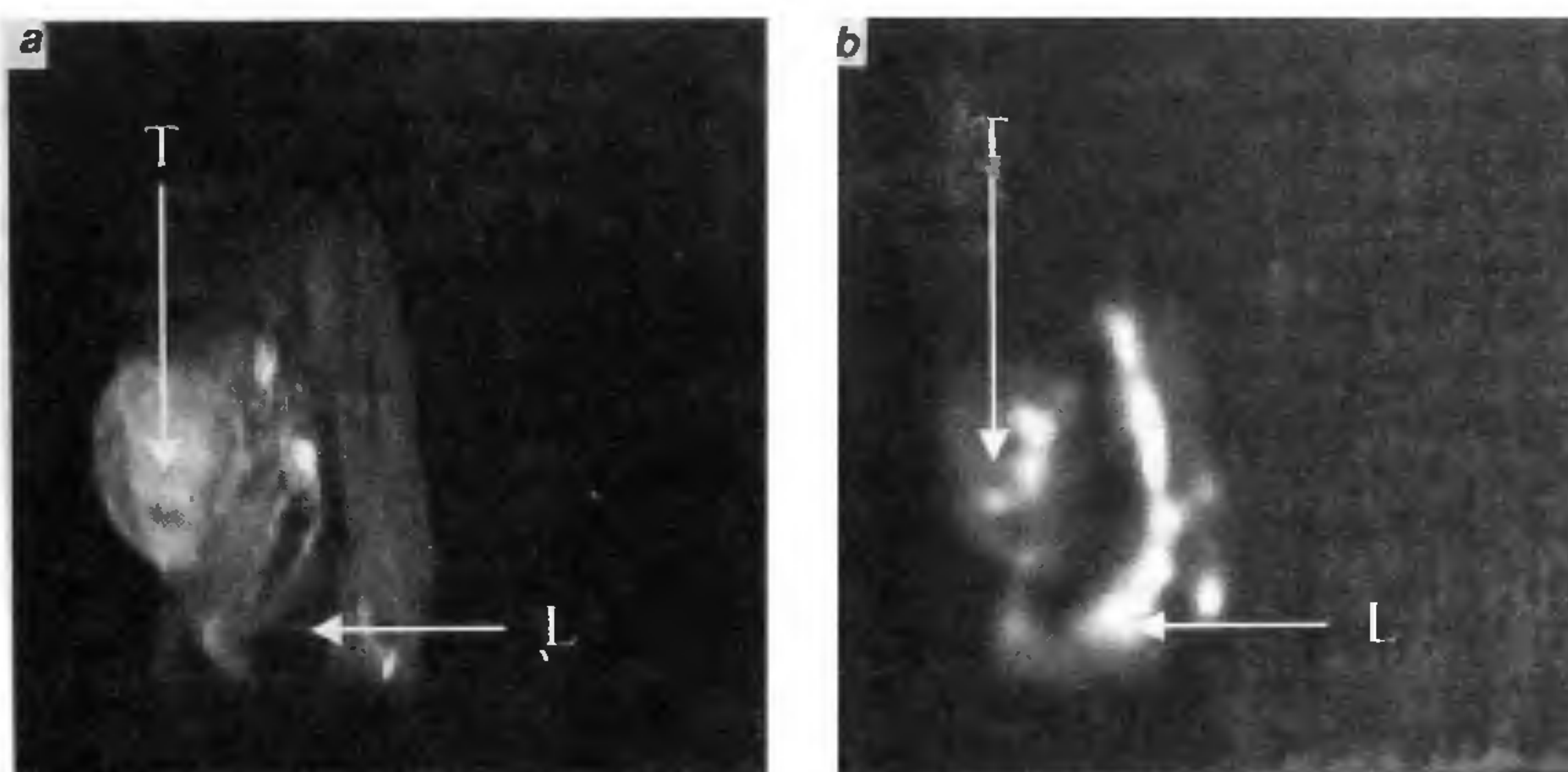


Figure 4. *a*, ^1H and *b*, ^{19}F whole-body images of a C_3H mouse bearing a RIF-1 tumour after i.v. administration of the perfluorocarbon Fluorovist, followed by 15 min breathing carbogen supplied at a rate of 2 l/min. The tumour uptake is much more homogeneous than in the absence of carbogen breathing, as may be seen by comparison with Figure 2. The ^{19}F image is the saturation-recovery image from a SUFIR dataset.

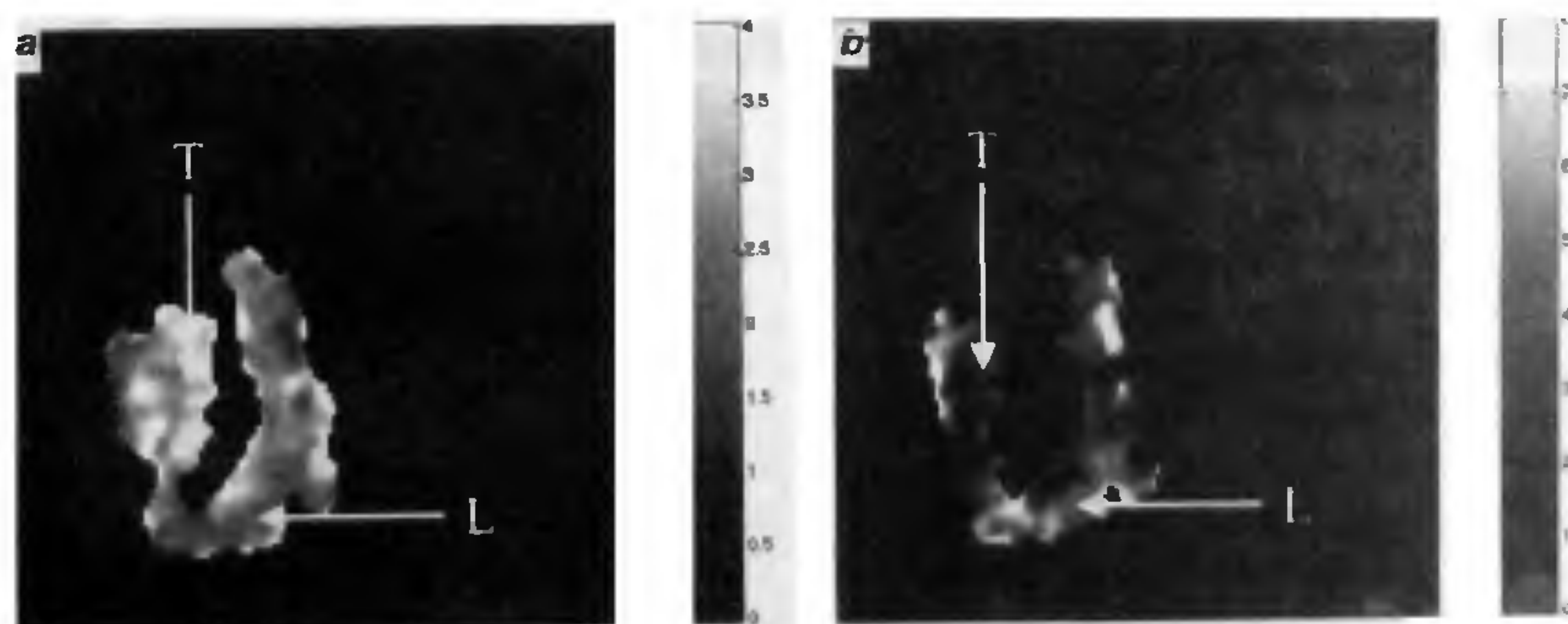


Figure 5. *a*, The T_1 map calculated from the ^{19}F SUFIR images obtained in the experiment illustrated in Figure 4. The scale bar is marked in seconds; *b*, The $p\text{O}_2$ map calculated from the T_1 map in *a*. The scale is in mm Hg.

lower than the levels observed in the liver and spleen (60 ± 7 and 81 ± 9 mm Hg respectively), but much higher than the Eppendorf microelectrode value of 1.3 mm Hg for these tumours¹⁶.

Carbogen thus appears to be an effective adjuvant for PFC imaging in about a quarter of RIF-1 tumours. Its effectiveness presumably depends on tumour vascularization. The enhancement by carbogen may be ascribed to temporary opening of the tumour vessels by the carbogen, PFC entering and then being trapped there by the closure of the vessels when air breathing is resumed. Because the amount of Fluorovist taken up into the RIF-1 tumours (assessed by SNR), even with carbogen breathing, was inadequate for over half of the experiments, just as it was for the PCE, we tried two other tumour models. The first was the GH3 tumour grown in nude mice. It had been shown in other experiments in our laboratory¹⁷ that this tumour model contained a vasculature that responded well to carbogen breathing, as assessed by an increase in signal intensity measured by GRE-MRI, and it therefore seemed a good candidate. However, similar to our experience with RIF-1 tumours, the amount of PFC taken up into the tumour was only adequate to give a SNR of $>> 30$ in 5 out of 13 animals. The average pO_2 during air-breathing from these 5 successful PFC measurements was 34 ± 7 mm Hg. Again, this is much higher than the pO_2 of this tumour type (2.8 mm Hg) measured by Eppendorf¹⁸. A representative set of images of this tumour type is seen in Figure 6. This animal underwent the carbogen breathing protocol. A proton scout image is shown in Figure 6a, and a fluorine image marked with the ROIs studied in Figure

6b. The baseline, carbogen supply on, and first recovery pO_2 maps are shown in Figure 6c, d and e respectively. pO_2 values measured from the ROIs are plotted in Figure 7 as mean \pm SEM over the ROI. The pO_2 in each rises during carbogen breathing. ROI 3 remains significantly elevated during the first 11 min of recovery.

The final tumour type tested was SAF sarcoma grown in CBA mice. 10 mice were given LV i.t. Two injections failed. In the remaining 8 animals, the tumour SNR was around 30 in all cases, which remains too low for accurate pO_2 imaging, though averaging over the entire tumour allows a mean pO_2 to be obtained. An example is shown in Figure 8. This animal underwent the carbogen/nicotinamide protocol, with two 25 min scans being acquired after the administration of nicotinamide. Averaging over the whole tumour gave measurements of 31.5 mm Hg during carbogen breathing, 36.5 mm Hg during the first scan after nicotinamide administration, and 46 mm Hg during the final scan. As before, all these values are much higher than the median (1.5 mm Hg) measured by Eppendorf¹⁶.

Generally, we observe that of three tumour types, the RIF-1 and the GH3 show inconsistent uptake, while the SAF shows consistent uptake which is at a level slightly too low to image pO_2 effectively. Additionally, we observe that the tumour pO_2 measured by PFC imaging is much higher than the median value measured by the Eppendorf electrode. A plausible explanation for this observation is that a small percentage of tumour cells have pO_2 values of up to 100 mm Hg as measured by Eppendorf. These are the cells that are closest to the larger tumour blood vessels, and it is likely that PFC adminis-

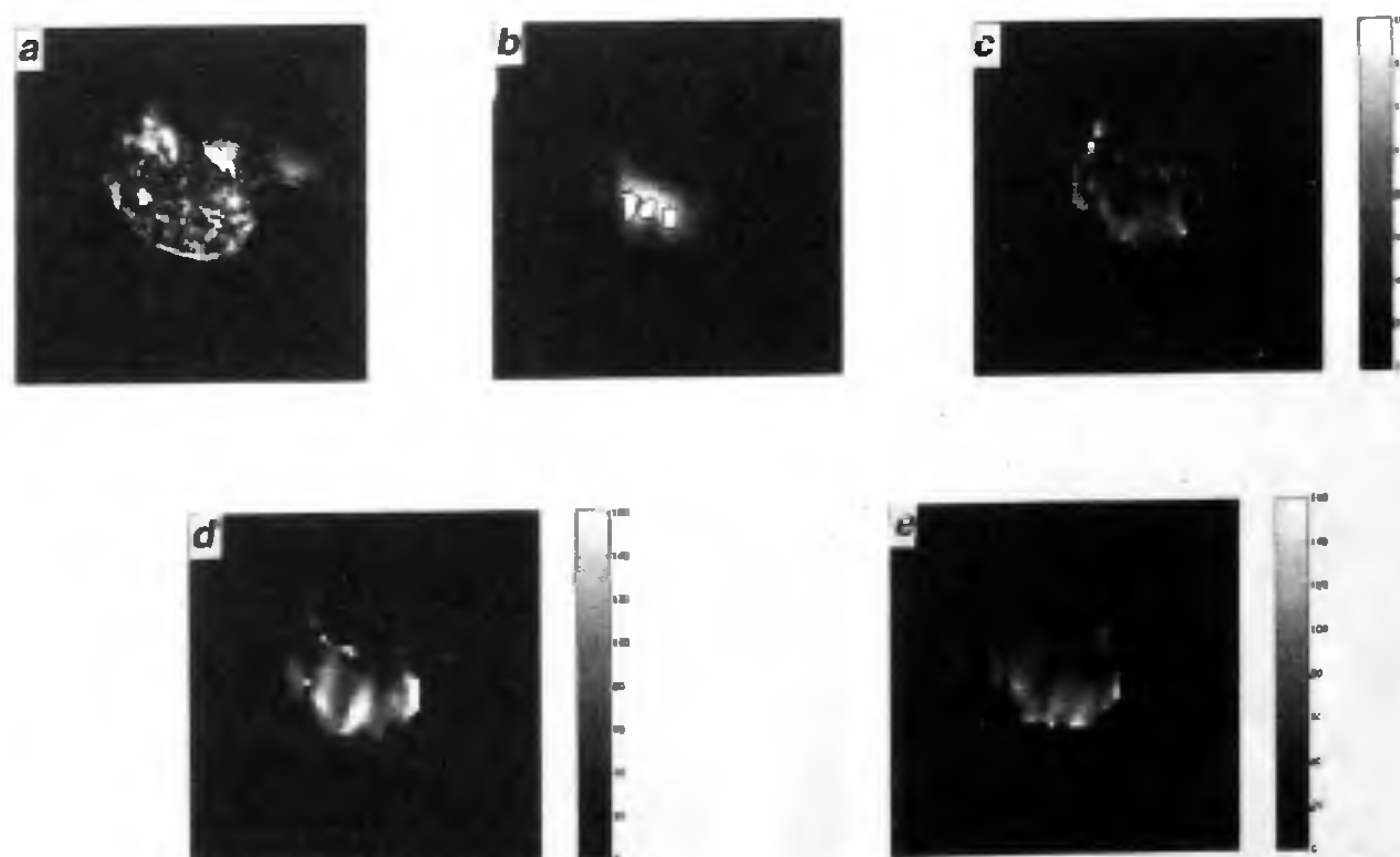


Figure 6. Images obtained from a nude mouse bearing a GH3 prolactinoma after i.v. administration of Fluorovist followed by 15 min of carbogen breathing. These images were obtained using a surface coil over the tumour. *a*, 1H scout image; *b*, sample ^{19}F image, with three ROIs marked as white spots ringed with black; *c*, baseline pO_2 map; *d*, pO_2 map obtained while the animal breathed carbogen for 11 min; *e*, pO_2 map obtained in the first 11 min of air-breathing after the carbogen supply was shut off. Four further pO_2 maps were obtained (see Figure 7).

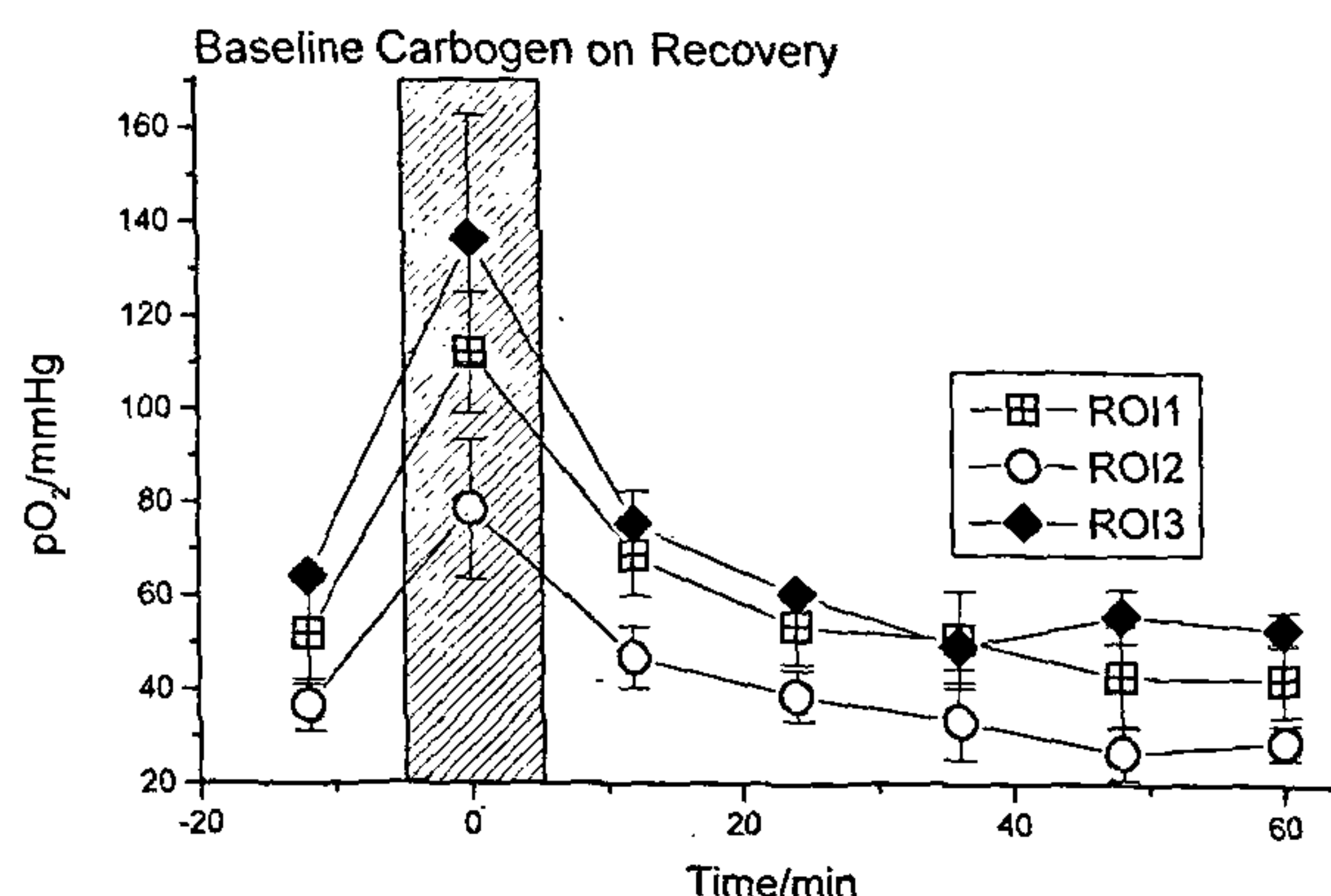


Figure 7. Graphs of the pO_2 values measured from the ROIs marked in Figure 6b for baseline (air breathing), carbogen breathing, and 55 min of recovery (air breathing). Values are mean \pm SEM over each ROI. Highly significant increases are seen during carbogen breathing. ROI 3 remains significantly elevated during the first 11 min of recovery.

tered i.v. will be sequestered in macrophages that are also close to the blood vessels. Hence, it is possible that we have accurately measured the pO_2 of a small fraction of cells which are well oxygenated, while neglecting the hypoxic majority of cells. We therefore embarked on intratumoural injection of PFC, intending to improve the sampling of hypoxic regions and increase the fraction of animals in which we could measure tumour pO_2 .

Measurements of intratumoural injections of hexafluorobenzene

Mason *et al.*¹⁹ have shown that hexafluorobenzene (HFB) administered by the intratumoural injection route is a sensitive indicator of tumour oxygenation. This method, which was developed at a field strength of 7 T (much higher than the 1.9 T field strength used in this study), only interrogates the pO_2 of the small volume covered by the injection site. On the other hand, it can interrogate poorly vascularized tumour regions that would be inaccessible by i.v.-delivered PFC. In the present study, 31 animals bearing GH3 tumours were injected with HFB and 5 with pure Fluorovist, by methods described earlier. Of these, 20 injected with HFB and 2 with Fluorovist showed sufficient residual tumour signal for accurate T_1 mapping to be possible. Representative data are shown in Figure 9. In general, even when 3 injections were given, usually only one or two would be visible in the images, the remainder leaking into the bloodstream. This leakage of pure, unemulsified PFC caused fetal embolisms in many animals. This problem could of course be eliminated by injecting emulsified PFC, as was used in the i.v. experiments. Measurements

of the SNR obtained after injecting into tumours of dead mice suggest that there is always partial leakage in the live animals, as the SNR is always significantly lower in living animals than in the dead mice. Serial studies of living mice show that up to 50% of the PFC remaining in the tumour immediately after injection will be lost in the next 48 h, and none remains after 5 days.

Baseline measurements were taken from all tumours in which the signal could be imaged; one ROI was measured for each droplet of PFC visible. For some animals, the carbogen protocol described earlier was applied. In this group, the ROIs observed can be divided into responders and non-responders to carbogen breathing. Sample data are plotted in Figure 10. The majority of the non-responders were hypoxic throughout, representing chronically hypoxic regions of the tumour which were unaffected by carbogen breathing. The responders included acutely hypoxic regions, which became oxygenated on carbogen breathing, and more normally oxygenated regions whose oxygenation increases for 10–20 min after cessation of carbogen breathing. These results were confirmed by a separate study using Fluorovist injected i.t. and monitored with a 5 min time resolution (results not shown), as opposed to the 11 min resolution of the HFB studies. Again, there was a delay in the pO_2 increase, and most of it occurred after the animal had ceased to breathe carbogen. This lag was consistent with observations in gradient-echo images in which the signal intensity was weighted by the deoxyhaemoglobin content of the tissue; in this tumour type the image brightness shows a lag both in brightening at the start of carbogen breathing and in returning to the baseline at the end of the breathing. The use of the scavenger made it unlikely that the delay was due to gas accumulation in the magnet bore.

The baseline measurements are plotted as a histogram in Figure 11. The mean value was 12.5 ± 2 mm Hg. Note that almost 50% of values are < 5 mm Hg, and the distribution is clearly hypoxic. The histogram resembles the one obtained by using the Eppendorf electrode, though with a smaller proportion of hypoxic values. It may be noted that the SNR of the images is reduced at lower pO_2 , so that a larger quantity of PFC is required for imaging to be possible, particularly for HFB where the maximum T_1 is 16 s, resulting in 80–95% attenuation of the signal with the parameters used. Hence, where the ROI is hypoxic, the data are more likely to be unmeasurable, which may account for this discrepancy. Nonetheless, the data are much closer to the Eppendorf values than when i.v. experiments are performed. This is not due to the use of HFB instead of Fluorovist, since the values obtained from Fluorovist injected i.t. were also hypoxic (1.83 ± 4 mm Hg).

In conclusion, the imaging sequence that we have demonstrated, in combination with blood-flow modification to enhance PFC uptake in experimental tumours,

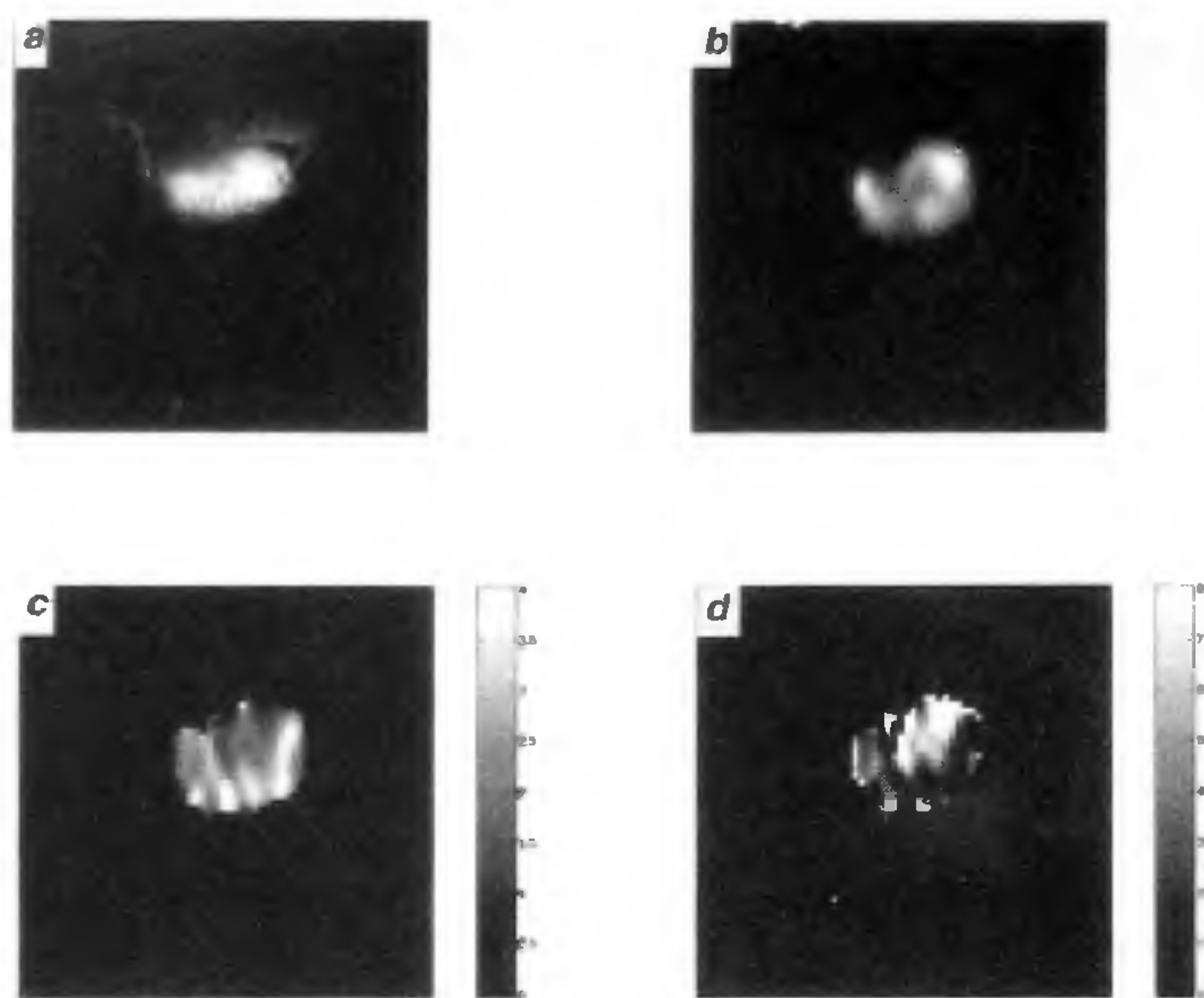


Figure 8. Images obtained from a CBA mouse bearing a SAF tumour after i.v. administration of Fluorovist followed by 15 min of carbogen breathing. *a*, ¹H scout image; *b*, ¹⁹F image; *c*, T₁ map with scale marked in seconds; *d*, pO₂ map with scale 0–80 mm Hg. The animal was breathing carbogen while this data was acquired.

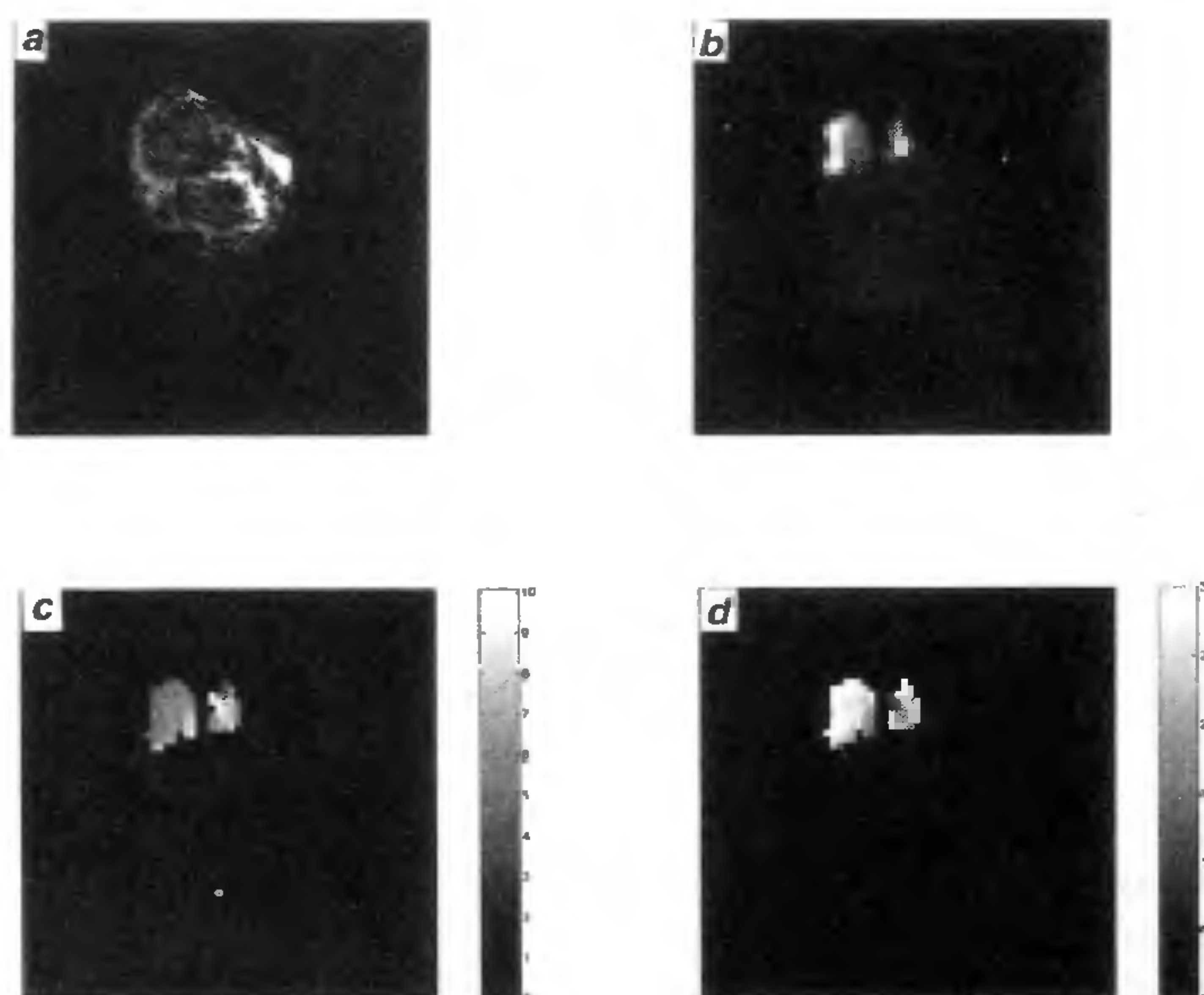


Figure 9. Images of a nude mouse bearing a GH3 tumour after i.t. administration of hexafluorobenzene. *a*, ¹H scout image; *b*, ¹⁹F image; *c*, T₁ map with scale marked in seconds; *d*, pO₂ map with scale 0–30 mm Hg. Two injected droplets are visible in this case.

allows PFC oxygen tension measurements in small tissue volumes. However, the success rate depends on the tumour type. Overall only about 25% of RIF-1 and 40% of

GH3 tumours take up enough i.v.-administered PFC for an adequate SNR to be achieved and for a pO₂ map to be constructed, and even then the homogeneity of the

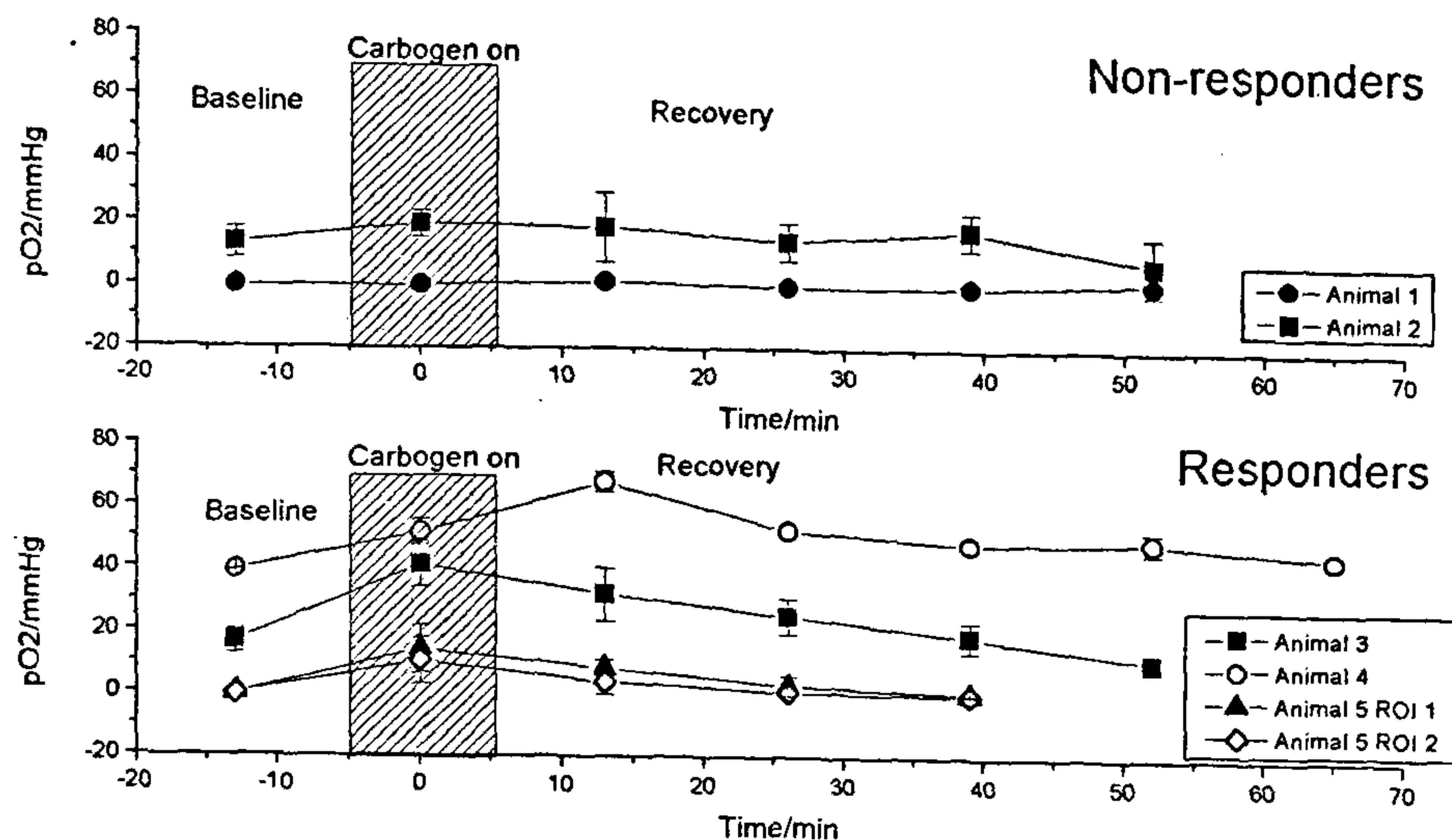


Figure 10. ^{19}F MRI $p\text{O}_2$ measurements displaying response to an episode of carbogen breathing in nude mice bearing GH3 tumours. Hexafluorobenzene was administered i.t. Note the significant delay in return to baseline for the responding ROIs.

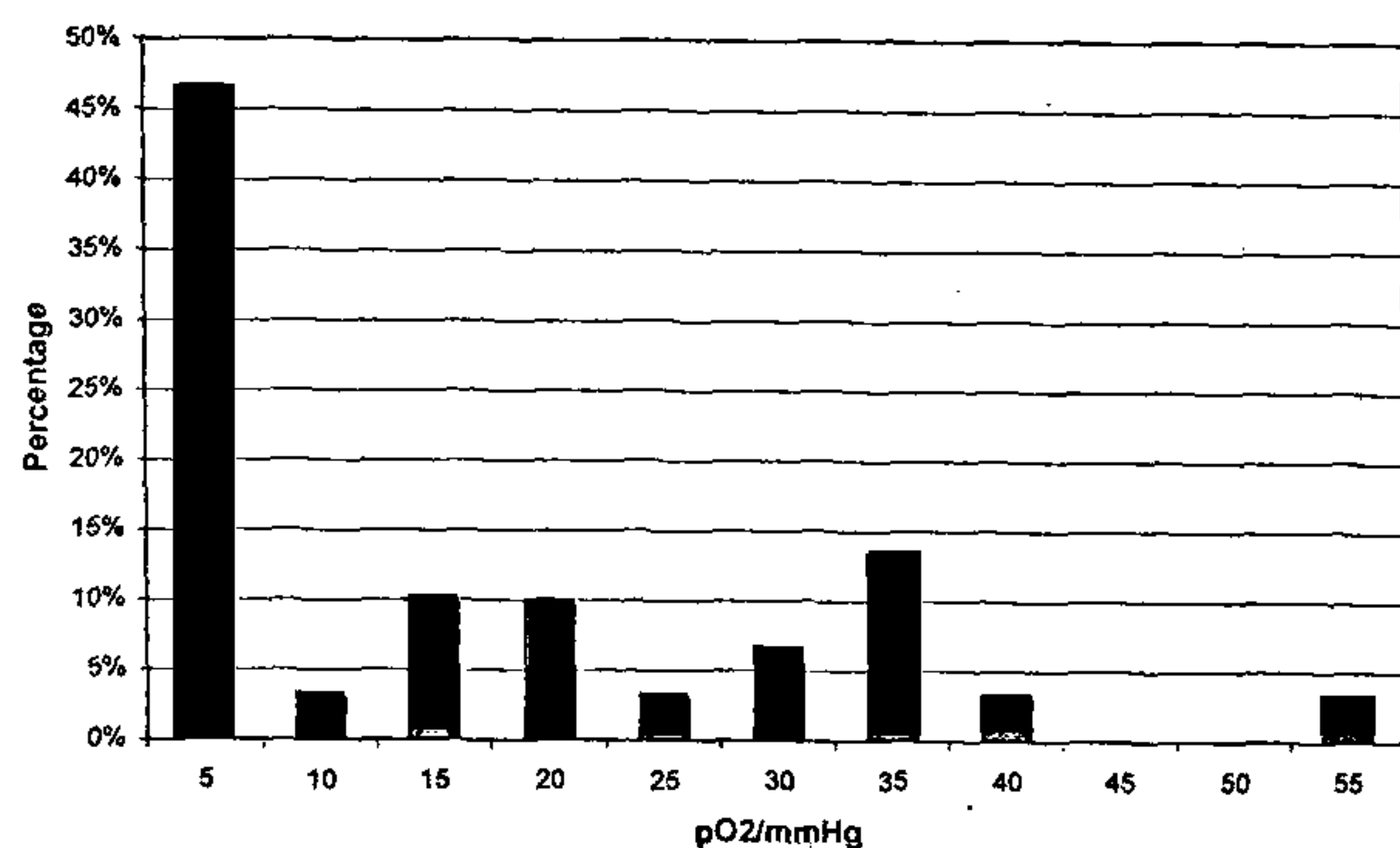


Figure 11. ^{19}F MRI $p\text{O}_2$ measurements of hexafluorobenzene administered i.t. to nude mice bearing GH3 tumours, displayed as a histogram whose distribution resembles those obtained by Eppendorf electrode.

uptake is poor. The homogeneity is somewhat improved by allowing the animals to breathe carbogen, but the proportion of successful uptake in RIF-1 was not increased (no studies were performed on GH3 tumours without carbogen breathing). Similar experiences have been communicated by van den Sanden (personal communication) who found sufficient PFC uptake in only one out of three tumour types. Additionally, the $p\text{O}_2$ values observed are higher than those observed by other methods. When sufficient PFC uptake is achieved, measurements of $p\text{O}_2$ in tumours can be made with a spatial resolution of $8 \times 1 \times 1 \text{ mm}^3$. The inconsistency

of i.v. administration may limit the clinical potential of PFCs, as many tumours are not readily injectable.

Better results may be obtained in animal models by using i.t. injection of PFC. In the GH3 tumour, measurable signal is obtained in 60% of tumours when i.t. injection is employed. Furthermore, the $p\text{O}_2$ values obtained are much more consistent with those measured using Eppendorf electrode. This may provide a useful method for measuring $p\text{O}_2$ *in vivo* to study blood flow modifiers and for radiobiological studies.

1. Thomlison, R. H. and Gray, L. H., *Br. J. Cancer*, 1955, 9, 539-549.
2. Hills, S. A., Collingridge, D. R., Vojnovic, B. and Chaplin, D. J., *Int. J. Radiat. Oncol., Biol. Phys.*, 1998, 40, 943-951.
3. Falk, S. J., Ward, R. and Bleehen, N. M., *Br. J. Cancer*, 1992, 66, 919-924.
4. Vaupel, P., Schlenger, K., Knoop, C. and Höckel, M., *Cancer Res.*, 1991, 51, 3316-3322.
5. Clark, L. C. and Gollan, F., *Science*, 1966, 152, 1755-1756.
6. Parhami, P. and Fung, B. N., *J. Phys. Chem.*, 1983, 87, 1928-1931.
7. Clark, L. C., Ackerman, J. L., Thomas, S. R. and Millard, R. W., *Magn. Reson. Med.*, 1984, 1, 135-136.
8. Mason, R. P., Nunnally, R. L. and Antich, P. P., *Magn. Reson. Med.*, 1991, 18, 71-79.
9. Thomas, S. R., in *Magnetic Resonance Imaging Volume 2: Physical Principles and Instrumentation* (eds Partain, Price, Patton, Kulkavani, James), 2nd edn., W. B. Saunders Co, Philadelphia, 1988.
10. Dardzinski, B. J. and Sotak, C. H., *Magn. Reson. Med.*, 1994, 32, 88-97.
11. Canet, D., Brondeau, J. and Elbayed, K., *J. Magn. Reson.*, 1988, 77, 483-490.
12. Rojas, A., *Radiother. Oncol.*, 1991, 20 (Suppl 1), 65-70.

13. Twentyman, P. R., Brown, J. M., Gray, J. W., Franko, A. J., Scoles, M. A. and Kallman, R. F., *JNCI*, 1980, **64**, 595-605.
14. Prysor-Jones, R. A. and Jenkins, J. S., *J. Endocrinol.*, 1981, **88**, 463-469.
15. Chaplin, D. J., Horsman, M. R. and Aoki, D. S., *Br. J. Cancer*, 1992, **66**, 919-924.
16. Collingridge, D. R., Ph D thesis, University of London; 1997.
17. Robinson, S. P., Rodrigues, L. M., Ojunga, A. S. E., McSheehy, P. M. J., Howe, F. A. and Griffiths, J. R., *Br. J. Cancer*, 1997, **75**, 1000-1006.
18. Robinson, S. P., Collingridge, D. R., Rodrigues, L. M., Howe, F. A., Chaplin, D. J. and Griffiths, J. R., *NMR Biomed.*, in press.
19. Mason, R. P., Rodbumrung, W. and Antich, P. P., *NMR Biomed.*, 1996, **9**, 125-134.

ACKNOWLEDGEMENTS. We thank Dr C. Sotak for helpful advice, and HemaGen, St. Louis, Mo, for supplying us with Fluorovist and PCE, Dr D. R. Collingridge for performing the oxygen electrode studies, Dr H. Baddeley and Dr M. I. Saunders for stimulating discussions, and Dr M. Stubbs for providing a critical review of the manuscript. D. J. M. thanks Dr A. M. Howseman, SMIS, for his assistance in programming the imaging sequence. This work was supported by the Cancer Research Campaign, grant no. SP1971/0402.